Food & Function

Accepted Manuscript

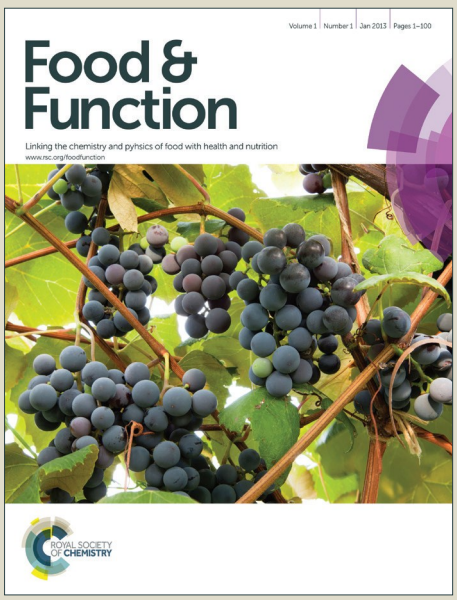

This is an *Accepted Manuscript*, which has been through the Royal Society of Chemistry peer review process and has been accepted for publication.

Accepted Manuscripts are published online shortly after acceptance, before technical editing, formatting and proof reading. Using this free service, authors can make their results available to the community, in citable form, before we publish the edited article. We will replace this *Accepted Manuscript* with the edited and formatted *Advance Article* as soon as it is available.

You can find more information about *Accepted Manuscripts* in the Information for Authors.

Please note that technical editing may introduce minor changes to the text and/or graphics, which may alter content. The journal's standard Terms & Conditions and the Ethical guidelines still apply. In no event shall the Royal Society of Chemistry be held responsible for any errors or omissions in this *Accepted Manuscript* or any consequences arising from the use of any information it contains.

ROYAL SOCIETY OF CHEMISTRY

www.rsc.org/foodfunction

Apigenin-7-O-*β*-D-glucuronide inhibits LPS-induced inflammation through the inactivation of AP-1 and MAPK signaling pathways in RAW 264.7 macrophages and protects mice against endotoxin shock

Weicheng Hu [a1], Xinfeng Wang [a 1], Lei Wu [b1], Ting Shen [a], Lilian Ji [a], Xihong Zhao [c], Chuan-Ling Si [b,d*], Yunyao Jiang [e], and Gongcheng Wang [f*]

[a] Jiangsu Collaborative Innovation Center of Regional Modern Agriculture & Environmental protection/Jiangsu Key Laboratory for Eco-Agricultural Biotechnology around Hongze Lake, Huaiyin Normal University, Huaian 223300, China.

[b] Tianjin Key Laboratory of Pulp & Paper, Tianjin University of Science & Technology, Tianjin 300457, China

[c] Key Laboratory for Green Chemical Process of Ministry of Education, School of Chemical Engineering and Pharmacy, Wuhan Institute of Technology, Wuhan 430073, Hubei, China

[d] State Key Laboratory of Tree Genetics and Breeding, Northeast Forestry University, Harbin 150040, China

[e] Department of Medical Biotechnology, College of Biomedical Science, Kangwon National University, Chuncheon 200-701, Korea

[f] Department of Gerontology, Huai'an First People's Hospital, Nanjing Medical University, 6 Beijing West Road, Huaian 223300, China

[1] These authors equally contributed to this work.

* Corresponding authors:

C. L. Si: E-mail: sichli@tust.edu.cn;

Tel: +86-22-60602006; Fax: +86-22-60602510

G. Wang: E-mail: wgc1955@sina.com;

Tel.: +86-517-80872307; Fax: +86-517-84922412.

Abstract

Apigenin-7-O-*β*-D-glucuronide (AG), an active flavonoid derivative isolated from the agricultural residue of *Juglans sigillata* fruit husks, possesses multiple pharmacological activities, including anti-oxidant, anti-complement, and aldose reductase inhibitory activities. To date, no report has that identified the anti-inflammatory mechanisms of AG. This study was therefore designed to characterize the molecular mechanisms of AG on lipopolysaccharide (LPS)-induced inflammatory cytokines in RAW 264.7 cells and on endotoxin-induced shock in mice. AG suppressed the release of nitric oxide (NO), prostaglandin E_2 (PGE_2), and tumour necrosis factor-*α* (TNF-*α*) in LPS-stimulated RAW264.7 macrophages in a dose-dependent manner without affecting cell viability. Additionally, AG suppressed LPS-induced mRNA expression of inducible nitric oxide synthase (iNOS), cyclooxygenase-2 (COX-2), and TNF-*α*. AG treatment decreased the translocation of c-Jun into the nucleus, and decreased activator protein-1 (AP-1)-mediated luciferase activity through inhibition of both p38 mitogen-activated protein kinase (MAPK) and extracellular signal-regulated kinase (ERK) phosphorylation. Consistent with the *in vitro* observations, AG protected mice from LPS-induced endotoxin shock by inhibiting proinflammatory cytokine production. Taken together, these results suggest that AG may be used as a source of anti-inflammatory agents as well as a dietary complement for health promotion.

Keywords: *Juglans sigillata*, apigenin-7-O-*β*-D-glucuronide, anti-inflammatory activity, cyclooxygenase-2, activator protein-1

1. Introduction

Inflammation is a physiological defence of the body's innate immune system against harmful stimuli such as pathogens, damaged cells, or irritants.[1] However, aberrant resolution and prolonged inflammation play significant roles in the pathogenesis of many diseases such as cancer, cardiovascular diseases, diabetes, skin disorders, Alzheimer's disease, and other inflammatory vascular diseases.[2,3] In particular, macrophages play a crucial role in the modulation of inflammatory responses and reactive oxygen/nitrogen species induced by proinflammatory factors, such as endotoxin-like lipopolysaccharide (LPS).[4] Overproduction of inflammatory mediators such as nitric oxide (NO), prostaglandin E_2 (PGE_2), tumour necrosis factor (TNF)-α, interleukin (IL)-1β, and interleukin 6 (IL-6) have been reported to be involved in this process.[5] These inflammatory events require upregulated activity of non-receptor-type tyrosine kinases such as spleen tyrosine kinase (Syk), Src, Janus kinase (JAK) 2, phosphoinositide 3-kinase (PI3K), and protein kinase B (Akt), as well as mitogen-activated protein kinases (MAPKs), including extracellular signal-regulated kinase (ERK), c-Jun N-terminal kinase (JNK), and p38.[6,7] Activation of these signaling molecules is linked to the activation of transcription factors such as nuclear factor (NF)-κB, cAMP response element-binding protein (CREB), interferon regulatory transcription factor (IRF)-3, and activator protein (AP)-1.[8] Current studies are therefore being directed toward the development of new drugs based on targeting specific events in these inflammatory processes.[9-11]

A large number of steroidal and nonsteroidal anti-inflammatory drugs are currently being used for the treatment of chronic inflammatory diseases. However, long-term administration of these anti-inflammatory agents may produce serious side effects, including gastrointestinal

ulcers, bleeding, colorectal cancer, and renal disorders.[12,13] Therefore; many studies are currently developing drugs to attenuate inflammatory responses that can be used for long periods with minimal side effects.[14,15]

Fruit husks and other forestry residues, which have been relatively underutilised, could be possible sources of novel bioactive compounds. The search for such compounds isolated from plants is an ongoing process, and is currently leading to new discoveries.[16] *Juglans sigillata* Dode is a member of the Juglandaceae family. It is a fast-growing deciduous tree indigenous to the mountain regions of Tibet, Sichuan, Yunnan, and Guizhou provinces in southwest China.[17] The seeds of *J. sigillata* are highly valued for their dietary nutrition, and its seed husks have long been used as folk medicine for the treatment of esophageal, gastric, cardiac, and lung cancers.[18] The husks of *J. sigillata* fruits, long been treated as an agricultural and food industry residue, are therefore a valuable resource for extracting potential value-added medicines, healthcare agents, and cosmetics. Previous investigation of *J. sigillata* fruit husks identified as α-tetralone derivatives.[19] However, to the best of our knowledge, this is the first report of apigenin-7-O-*β*-D-glucuronide (AG) from this tree. More importantly, the mechanism(s) responsible for the anti-inflammatory effects of AG from these husks are not known. In the following study, we characterized the anti-inflammatory mechanism(s) of AG using both *in vitro* and *in vivo* model systems involving the inflammatory response induced by LPS treatment.

2. Materials and methods

2.1. Plant material and chemicals

Fresh husks of *J. sigillata* fruits were gathered at Santai County, Yunnan Province, China in October 2008, and were authenticated by Prof. Dan Wang at Institute of Chemical Industry of Forest Products, Chinese Academy of Forestry, China. A voucher specimen (CMSCE-081006) was deposited at the herbarium of Tianjin Key Laboratory of Pulp and Paper, Tianjin University of Science and Technology, China. The supplies of sulfanilamide, naphthylethylenediamine dihydrochloride, LPS (*E. coli* 0111:B4), NG-monomethyl-L-arginine (L-NMA), and 1-(4,5-dimethylthiazol-2-yl)-3,5-diphenylformazan (MTT) were purchased from Sigma (St. Louis, MO). SB203580 and PD98059 were purchased from Calbiochem (San Diego, CA). The kit for RNA isolation and the first-strand cDNA synthesis were obtained from Invitrogen (Carlsbad, CA). The RPMI medium 1640, trypsin-EDTA, and antibiotics were acquired from Gibco BRL (Life Technologies, China). Fetal bovine serum (FBS) was acquired from Gibco BRL (Grand Island, NY). All culture supplies were obtained from the BD-Falcon brand (BD, Franklin Lakes, NJ). The reporter plasmids NF-κB-LUC and AP-1-LUC were purchased from Stratagene (La Jolla, CA). The phospho-specific ERK, c-Jun N-terminal kinase (JNK), IκBα, p38 mitogen-activated protein kinase (p38 MAPK), and the total antibodies to ERK, JNK, IκBα, p38 MAPK, and β-actin were obtained from Cell Signaling Technology (Beverly, MA). Antibody binding was measured using the enhanced chemiluminescence (ECL) Western blotting substrate (ComWin Biotech, China). All other chemicals were of analytical grade.

2.2. General Experimental

Open column chromatography (OCC) was carried out with Sephadex LH-20 and silica gel (Merck) as packing materials. Eluents were collected with a fraction collector (SBS-160). In TLC performance, DC-Plastikfolien Cellulose F (Merck, Darmstadt, Germany) plates were used and *t*-BuOH-HOAc-H_2O (3:1:1, v/v/v, solvent A) and HOAc-H_2O (3:47, v/v, solvent B) were used as developing solvents. TLC spots detection was conducted by UV light exposure (254 and 365 nm) and by spraying with 1% ethanolic $FeCl_3$ solution followed by heating. ^1H and ^{13}C NMR spectra were recorded in $(CD_3)_2SO$ with TMS as an internal standard on a Bruker Avance DPX 400 spectrometer at frequency of 400 and 100 MHz, respectively. Positive fast atom bombardment mass (FAB-MS) spectroscopy at measured with a Micromass Autospec M363 instrument.

2.3. Extraction and Purification

The air-dried and finely powdered fruit husks of *J. sigillata* (3.15 kg) were extracted five times in a jar (20 l) with 70% aqueous acetone (v/v) for more than four days at room temperature. The aqueous residues were combined, concentrated under vacuum, and then sequentially fractionated to give soluble fractions of *n*-hexane, $CHCl_3$, *n*-BuOH and H_2O, respectively. A portion of the above resulted H_2O-soluble fraction powder (25.60 g) was subjected to an OCC packing with silica gel with a gradient of $CHCl_3$-MeOH as the solvent system (39:1→3:1, v/v, 4000 ml) to produce five fractions, which were guided and grouped by TLC experiments. Then the third fraction $JSHW_3$ (8.25 g) was further loaded over an OCC packing with Sephadex LH-20 and eluting with MeOH-H_2O (2:1, v/v, 2000 ml) to give three fractions $JSHW_{31}$, $JSHW_{32}$ and $JSHW_{33}$. $JSHW_{32}$ (3.06 g) was also chromatographed on a

Sephadex LH-20 open column with repeated MeOH-H_2O (1:2 and 1:6, v/v, 1000 and 800 ml, respectively) to yield a yellow amorphous compounds (1, 122.4 mg).

Apigenin-7-*O*-*β*-D-glucuronide (**1**): Yellow amorphous powder; R_f: 0.50 (solvent A) and 0.06 (solvent B); Positive FAB-MS *m/z*: $[M+H\text{-}GluA]^+$ at 271 and $[M+H]^+$ at 447. ^{1}H-NMR (400 MHz, *δ*, $(CD_3)_2SO$): 3.68 (3H, *m*, H-2", 3", 4"), 4.06 (1H, *d*, *J* = 8.1 Hz, H-5"), 5.19 (1H, *d*, *J* = 6.1 Hz, H-1"), 6.52 (1H, *d*, *J* = 1.9 Hz, H-6), 6.73 (1H, *d*, *J* = 1.9 Hz, H-8), 6.90 (1H, *s*, H-3), 7.12 (2H, *d*, *J*=8.2 Hz, H-3', 5'), 7.80 (1H, *d*, *J*=8.2 Hz, H-2', 6'); ^{13}C-NMR (100 MHz, *δ*, $(CD_3)_2SO$): 70.2 (C-4"), 75.6 (C-3"), 76.6 (C-5"), 73.9 (C-2"), 94.3 (C-8), 99.6 (C-1"), 99.8 (C-6), 103.4 (C-3), 105.7 (C-10), 116.8 (C-3',5'), 121.9 (C-1'), 129.4 (C-2',6'), 157.6 (C-9), 161.8 (C-5), 162.8 (C-4'), 163.4 (C-7), 164.8 (C-2), 173.5 (C-6"), 182.8 (C-4).

2.4. Cell line and cell culture

The RAW 264.7 cell line was purchased from the American Type Culture (Manassas, VA). The RAW 264.7 cells were maintained in RPMI 1640, supplemented with L-glutamine (2 mM), 10% heat-inactivated FBS, 100 U ml^{-1} of penicillin, and 100 μg ml^{-1} of streptomycin. Cells were incubated at 37°C in a 5% CO_2 humidified atmosphere (MCO-15AC CO_2 incubator, SANYO, Osaka, Japan).

2.5. Cell viability assay

The cytotoxicity of AG on the RAW 264.7 cells was investigated by MTT assay.[20] RAW 264.7 cells were incubated in 96-well cell plate with a density of 1×10^5 cells $well^{-1}$ overnight and then exposed to the medium in the presence of different concentrations of AG for 24 h.

Subsequently, the supernatants were carefully aspirated from each well. Then, a total of 10 µl of MTT solution [5 mg ml^{-1} in phosphate-buffered saline (PBS)] and 90 µl of FBS-free medium were added to each well for another 3 h. The dark blue formazan crystals formed inside the intact mitochondria were solubilized with 100 µl of MTT stop solution [containing 10% sodium dodecyl sulfate (SDS) and 0.01 M hydrochloric acid]. The optical density was measured at 550 nm using an Infinite M200 Pro spectrophotometer (Tecan, Switzerland). The experiments were repeated in triplicate, three times independently. The data are expressed as mean percentages of the viable cells compared to the respective control.

2.6. Determination of NO, PGE_2, and TNF-α production

RAW 264.7 cells were plated in a 96-well cell plate with 1×10^5 cells $well^{-1}$ and allowed to adhere overnight. Then, medium was removed and pretreated with different concentrations of AG or positive control (L-NMA) for 30 min, followed by stimulated with LPS (1 µg/ml) for an additional 24 h. The aliquots of 100 µl of the cell culture medium were mixed with an equal volume of Griess reagent (1% sulfanilamide in 5% phosphoric acid and 0.1% naphthylethylenediamine dihydrochloride) in a separate 96-well plate and incubated at room temperature for 5 min. The absorbance was measured at 550 nm using an Infinite M200 Pro spectrophotometer. Fresh culture media were used as blanks in all experiments and NO production by LPS stimulation was designated as 100% for each group. The production of PGE_2 and TNF-α in the supernatant was quantified using the enzyme immunoassay kits (R&D Systems, MN) according to the manufacturer's instructions. The production of PGE_2 and TNF-α were measured relative to that of the control.

2.7. RNA extraction and reverse transcription-polymerase chain reaction (RT-PCR)

A total of 5 × 10^6 cells were plated per well in 60-mm cell culture plates with 4 ml culture medium for 16 h and exposed to different concentrations of AG for 30 min, followed by treatment with LPS and incubation for additional 6 h. RT-PCR was done as described previously with minor modification.[21] Total RNA was isolated using the Trizol reagent (Invitrogen, Carlsbad, CA). The concentration and purity of RNA was measured with a UV spectrophotometer (Nanodrop 2000c, Thermo Scientific, Wilmington, DE). The total RNA (2 μg) was incubated with oligo-dT15 and dNTPs for 5 min at 65 °C, and then transferred to ice, mixed with a 5 × first-strand buffer, RNase inhibitor, and 0.1 M DTT. The reaction mixture was further incubated for 2 min at 37 °C and for 1 h after the addition of M-MLV reverse transcriptase reverse transcriptase. The reaction was stopped by heating at 70 °C. The following primers (Generay Biotech Co., Ltd, Shanghai, China) were used for the amplification of GAPDH, iNOS, COX-2, and TNF-α: 5'-CACTCACGGCAAATTCAACGGCA-3' and 5'-GACTCCACGACATACTCAGCAC-3' for GAPDH, 5'-CCCTTCCGAAGTTTCTGGCAGCAG-3' and 5'-GGCTGTCAGAGCCTCGTGGCTTTGG-3' for iNOS, 5'-CACTACATCCTGACCCACTT-3' and 5'-ATGCTCCTGCTTGAGTATGT-3' for COX-2, and 5'-CCTGTAGCCCACGTCGTAGC-3' and 5'-TTGACCTCAGCGCTGAGTTG-3' for TNF-*α*. The condition for semi-quantitative PCR was 94 °C for 5 min followed by 25 (GAPDH and iNOS), 20 (COX-2), or 30 (TNF-*α*) cycles of 94 °C for 60 s, 55 °C for 60 s, and 72 °C for 90 s, with a final extension at 72 °C for 7 min. The amplified products were separated by 1%

agarose gel electrophoresis. The gels were stained with ethidium bromide and photographed with a Gel Doc XR system (Bio-Rad Laboratories, Hercules, CA). Quantification of mRNA was performed using real-time RT-PCR with manufacturer's instructions of SYBR Premix Ex Taq (TaKaRa, Dalian, China) using real-time thermal cycler (Bio-Rad, Hercules, CA). The real-time RT-PCR amplifications were carried out on a 96-well plate in the total volume of 40 μl containing 25 μl SYBR Premix Ex Taq, 4 μl cDNA template, 1 μl ROX reference dye, 1 μl each of forward and reverse primer and 9 μl distilled water. The condition for real-time PCR was 94 °C for 10 min followed by 30 cycles at 94 °C for 15 s, 55 °C for 15 s, and 72 °C for 30 s, with a final extension at 72 °C for 1 min. Relative expression levels of the target genes were calculated from $2^{-\Delta\Delta CT}$.

2.8. Transfections and luciferase assay

The RAW 264.7 cells (5×10^5 cells ml^{-1}) were seeded to 12-well plates to maintain approximately 70–80% confluence. Prior to transfection, cells were washed three times in 1 ml of Opti-MEM and 0.4 μg of plasmids containing NF-κB or AP-1 as well as *β*-galactosidase were transfected using the Lipofectamine 2000 (Invitrogen, CA). After 24 h, the medium was replaced by complete PRMI-1640 and the transfected cells were treated with test samples in the presence or absence of LPS. Luciferase and *β*-galactosidase enzyme activities were performed using the luciferase assay system according to the procedure provided by the manufacturer (Promega, Madison, WI). Luciferase activity was normalized by *β*-galactosidase activity.

2.9. Cell lysis and imunoblotting

A total of 5×10^6 cells was plated per well in 60-mm cell culture plates for 16 h and then exposed to AG for 30 min before stimulation with LPS for indicated time. After washed twice with cold PBS, cells were harvested by scraping. Cell pellets were lysed in 200 μl lysis buffer (20 mM Tris-HCl, pH 7.4, 2 mM EDTA, 2 mM ethyleneglycotetraacetic acid, 50 mM *β*-glycerophosphate, 1 mM sodium orthovanadate, 1 mM DTT, 1% Triton X-100, 10% glycerol, 10 μg ml^{-1} aprotinin, 10 μg ml^{-1} pepstatin, 1 mM benzimide, and 2 mM hydrogen peroxide). Cell lysates were centrifuged at 12,000 g for 5 min at 4 °C. The supernatant was collected and concentration of protein was determined by enhanced bicinchoninic acid (BCA) protein assay kit (ComWin Biotech, China). Followed the treatment, the nuclear protein was extracted using nuclear protein isolation kit (ComWin Biotech, China). The procedures were as described previously.[22] Equal amounts of protein were boiled at 95 °C for 5 min and separated on a sodium dodecyl sulfate-polyacrylamide gel and transferred to polyvinylidene difluoride (PVDF; Bio-Rad) membranes. The membranes were blocked in blocking buffer (Tris-buffered saline containing 3% BSA, 20 mM NaF, 2 mM EDTA, and 0.2% Tween 20) for 1 h in at room temperature. The membrane was incubated for 1 h with the appropriate primary antibody at room temperature, and then washed three times with the TBST buffer (Tris-buffered saline containing 20 mM NaF, 2 mM EDTA, and 0.2% Tween 20), incubated further for 1 h with horseradish peroxidase (HRP)-conjugated goat immunoglobulin G and washed three times with TBST buffer. Bound antibodies were detected by ECL system and blots were observed with the Tanon-5200 chemiluminescence detection (Tanon Science, China).

2.10. *In vivo* endotoxin shock model

C57BL/6 mice weighing 20–22 g were obtained from Laboratory Animal Service Center of Yangzhou University and housed at a room temperature of 20 °C–25 °C under relative humidity (50 ± 10%) with a 12 h light/12 h dark cycle. All animals were allowed free access to a commercial stock diet and water throughout the experiment. All experiments were performed in accordance with guidelines established by the Animal Care and Use Committee of Nanjing Medical University. The C57BL/6 mice were injected intraperitoneally (i.p.) with LPS (20 mg kg^{-1}) dissolved in 10 mM cold sodium citrate buffer. AG (5 or 10 mg/kg) was administered (i.p.) 2 h before LPS challenge. Survival was monitored over the next 84 h and the blood samples were collected 12 h after LPS injection. Blood was allowed to clot, and serum was separated by centrifugation at 3000 rpm for 15 min. The levels of TNF-α and IL-1β were estimated using standard kits.

2.11. Statistical analysis

The data are expressed as the mean ± standard deviation (SD). Each experiment was repeated at least 3 times. One-way analysis of variance (ANOVA) was used to determine the significant differences between the groups, followed by a Duncan's multiple range test or Student's t-test. The *p*-values of less than 0.05 were considered as significant. All analyses were performed using SPSS 20 (SPSS Inc., Chicago, IL).

3. Results and discussion

3.1. Elucidation of chemical structure of isolated compound

Compound **1**, obtained as a yellow amorphous powder, gave a dark brown spot on a cellulose plate by spaying with ethanolic $FeCl_3$ and its R_f values were 0.50 (solvent A) and 0.06 (solvent B). It gave $[M+H]^+$ and $[M+H\text{-}GluA]^+$ ions at *m/z* 447 and 271, respectively, in positive FAB-MS spectrum, which was consistent with the molecular formula $C_{21}H_{18}O_{11}$. In the ^{1}H-NMR spectrum, an AA'BB' system constituted by two doublets (J = 8.2 Hz) at δ 7.12 and δ 7.80 attributable to H-3',5' and H-2',6' due to a *para*-substituted B ring. The *meta* coupling of H-6 and H-8 on phloroglucinol A ring presented at δ 6.52 (*d*, J = 1.9 Hz) and 6.73 (*d*, J = 1.9 Hz) respectively. The singlet of 3-H of heterocyclic C ring was observed at δ 6.90. The presence of a β-configuration glucuronic acid was evidenced by an anomeric proton doublet (J = 6.1 Hz) at δ 5.19, together with four protons ranging between δ 3.68 and 4.06. In ^{13}C-NMR spectrum, the sugar's carboxyl carbon typically resonance at δ 173.5 indicating a glucuronic acid moiety. In the HMBC spectrum, long range correlations were observed between the anomeric proton signal (δ 5.19) of glucuronic acid and C-7 of the aglycon (δ 163.4) demonstrating the linkage at the C-7 of apigenin. Thus, compound **1** was elucidated as apigenin-7-*O*-β-D-glucuronide.[23,24] To the best of knowledge, this is the first report of this compound from *Juglans* genus.

3.2. AG decreases LPS-induced release of NO, PGE_2, and TNF-α

Inflammation is a physiological function that is initiated in response to bacterial infection or tissue damage. This inflammatory reaction involves complicated networking, and is usually mediated by immune cells such as monocytes and macrophages.[25,26] During inflammation,

activation of macrophages results in the secretion of a series of proinflammatory mediators, including NO, PGE_2, and TNF-α, which help the immune cells escape from the bloodstream.[27] NO, synthesized from L-arginine by inducible nitric oxide synthase (iNOS), is a key inflammatory mediator that plays an important role in various types of inflammatory processes. TNF-α is an important inflammatory mediator that can elicit acute inflammatory diseases and cause tissue destruction.[28] Thus, reduction of LPS-induced proinflammatory cytokines in macrophages may represent an effective strategy for the development of novel anti-inflammatory agents.

A large number of flavonoids have been shown to possess anti-inflammatory properties based upon their abilities to scavenge reactive oxygen and nitrogen species. Sulfuretin, a flavonoid isolated from the heartwood of *Rhus verniciflua*, inhibits LPS-induced iNOS, COX-2, and proinflammatory cytokine expression via the downregulation of NF-κB in RAW 264.7 murine macrophage cells.[29] Kolaviron, a natural flavonoid from the seeds of *Garcinia kola*, reduces LPS-induced inflammation in macrophages by inhibiting IL-6 secretion and inflammatory transcription factors ERK1/2, NF-κB, p38, Akt, p-c-Jun, and JNK.[30] Isoliquiritigenin, isolated from the roots of *Glycyrrhiza uralensis,* inhibits LPS-induced iNOS and COX-2 expression via the attenuation of NF-κB in RAW 264.7 macrophages.[31]

AG is an active flavonoid derivative isolated from the agricultural residue of *J. sigillata* fruit husks. This flavonoid possesses multiple biological activities, including anti-oxidant, anti-complement, and aldose reductase inhibitory activities.[32-34] To date, there have been no reports describing the anti-inflammatory mechanisms of AG. The present study was therefore undertaken to characterize the pharmacological effects and mechanisms of AG in

LPS-stimulated macrophage-like RAW 264.7 cells and in an LPS-induced septic shock model. First, to determine the appropriate concentrations of AG, cell viability was measured by the MTT assay following exposure to AG. As shown in Figure 2A, the viabilities of RAW 264.7 cells were 104.97 ± 3.26%, 100.15 ± 9.90%, 97.92 ± 0.64%, and 94.42 ± 9.81% after exposure to 12.5, 25, 50, and 100 μM AG, respectively, for 24 h. Based upon these results, cells were incubated with AG at concentrations less than 100 μM for all subsequent experiments. LPS, one of the most powerful activators, binds to the CD14/TLR4 receptor complex and stimulates macrophages to secrete overproduced proinflammatory cytokines. To determine whether AG possesses anti-inflammatory activities, multiple proinflammatory mediators induced by LPS were monitored in RAW264.7 cells. As shown in Figure 2B, NO significantly accumulated in the media following LPS stimulation for 24 h; however, AG and NG-methyl-L-arginine (L-NMA) (a nonspecific iNOS blocker) suppressed NO production in a dose-dependent manner, with IC_{50} values of 62.48 μM and 92.26 μM, respectively (Fig. 2B). The results showed that AG inhibited NO production more efficiently than L-NMA. In addition, the inhibitory efficiency of this positive control was comparable with previous studies, indicating that our experimental conditions were valid. In agreement, a lot of scientific evidence supports the ethnopharmacological significance of apigenin derivatives with different efficacy in immune models.[35-37] Moreover, we also found that apigenin-7-O-(*β*-D-glucuronopyranosyl(1→2)-O-*β*-D-glucuronide didn't show any effect on LPS-stimulated RAW 264.7 cells (data not shown). We can see that, for apigenin, the addition of a glucuronic acid residue could remain its inflammatory activity. However, two glucuronoic acid units attached to apigenin decreased its anti-inflammatory property. It's indicated that the

inflammatory activities among apigenin and its derivatives are complex and it provided the impetus for further studies to delineate the structure-activity relationship of apigenin and its derivatives. We further investigated the effect of AG on the secretion of PGE_2 and TNF-α in LPS-stimulated RAW264.7 cells using an ELISA. As shown in Figures 2C and D, treatment with AG resulted in a dose-dependent inhibition of cytokine secretion, indicating that AG was able to inhibit the inflammatory response in macrophage cells.

3.3. AG inhibits LPS-induced iNOS, COX-2, and TNF-α expression

The secretion of inflammatory mediators requires a complicated signaling cascade for transcriptional activation of inflammatory genes.[38] iNOS activation occurs predominantly in activated macrophages, and can be induced by proinflammatory cytokines to cause NO accumulation in the cell supernatant.[39] COX-2 is the rate-limiting enzyme involved in the conversion of PGE_2 from arachidonic acid.[40] Hence, mRNA expression levels for this key enzyme and cytokines are logical targets for the development of novel anti-inflammatory agents. To determine whether AG-mediated inhibition of proinflammatory cytokines is regulated at the transcriptional level, RAW 264.7 cells were preincubated with AG for 30 min and then stimulated with LPS for 6 h. Semi-quantitative reverse transcription polymerase chain reaction (RT-PCR) (Fig. 3A) and real-time polymerase chain reaction (Fig. 3B) showed that the levels of iNOS, COX-2, and TNF-α mRNA expression in the unstimulated RAW 264.7 cells were low; however, these mRNA levels were upregulated by LPS, consistent with previous reports.[41,42] Pretreatment with AG strongly suppressed LPS-stimulated iNOS, COX-2, and TNF-α expression. Moreover, AG alone did not affect mRNA expression compared to the control group

(data not shown). Taken together, these results suggest that the effects of AG are at the transcriptional level.

3.4. AG inhibits activator protein-1 (AP-1)-induced nuclear translocation and MAPK phosphorylation

It is well-known that, during inflammation, AP-1 and NF-κB play important roles in the regulation of iNOS, COX-2, and TNF-α gene expression.[43] Therefore, we used immunoblot analyses and reporter gene assays to examine whether the reduction in mRNA levels was associated with nuclear translocation of c-Jun, c-fos, and NF-κB. As shown in Figure 4A, nuclear levels of c-Jun were decreased by AG treatment, without affecting levels of cytosolic proteins, as confirmed by levels of cytosolic β-tubulin. In agreement with these results, cells transfected with a luciferase reporter construct for AP-1 and NF-κB produced strong luciferase activity following stimulation by LPS, indicating that LPS activated AP-1- and NF-κB-mediated transcription in RAW 264.7 cells, whereas AG abrogated the activation of AP-1 (Figs. 4B and C). Induction of AP-1 activity is known to be triggered by ERK, p38 MAPK, and JNK, suggesting that MAPK signaling pathways are crucial for the regulation of AP-1 activity.[44] AP-1 complex is composed of a heterogeneous set of dimeric proteins, including Jun (c-Jun, JunB, and JunD) and Fos (c-Fos, FosB, Fra-1, and Fra-2) families. It was confirmed that c-Jun but not c-Fos is part of this complex at the AP-1 site in RAW 264.7 cells.[45] Taken together, our findings suggest that AG exert their anti-inflammatory effects by suppressing AP-1, which lead to the inhibition of NO, PGE_2 and TNF-α production in RAW 264.7 cells.

Signaling cascades that include MAPKs and PI3K/Akt are activated by LPS through binding

to its TLR4 receptor on cell membranes, leading to the regulation of inflammatory mediators.[46] MAPKs are members of a highly conserved family of protein serine/threonine kinases composed of three subtypes: JNK, ERK, and p38 kinase.[47] Once activated, MAPKs regulate the functional responses of cells through phosphorylation of transcription factors and stimulation of downstream signaling pathways.[48] In addition to MAPKs, when macrophages are activated by inflammatory stimuli, phosphorylated IκBα in the cytosol is translocated with the NF-κB p65 subunit into the nucleus.[49] Previous studies have reported that increases in p38, ERK, and IκBα led to the activation of redox-sensitive transcription factors (e.g., NF-κB and AP-1), and have further suggested that the MAPKs and PI3K/Akt signaling pathways directly facilitate DNA-binding activity, leading to upregulation of iNOS and TNF-α mRNA expression in RAW 264.7 cells.[50,51] For example, carabrol suppresses LPS-induced iNOS expression by inactivation of p38 and JNK via inhibition of IκBα degradation in RAW 264.7 cells.[52] Vitisin A suppresses LPS-induced NO production by inhibiting ERK, p38, and NF-κB activation in RAW 264.7 cells.[53] Suppression of iNOS and COX-2 expression by flavokawain A involves inhibition of NF-κB and AP-1 activation in RAW 264.7 cells,[54] and fucoxanthin inhibits the inflammatory response by suppressing the activation of NF-κB and MAPKs in LPS-induced RAW 264.7 cells.[55] Moreover, it has been demonstrated that specific MAPK inhibitors (e.g., SB203580, PD98059, and SP10065) suppress the expression of iNOS and COX-2.[56,57]

Based upon these results, it is possible that upstream signaling molecules are involved in AG inhibition of LPS-induced inflammation. Therefore, MAPKs and PI3K/Akt pathways were selected to determine whether AG was able to modulate upstream signaling events. RAW 264.7 cells were preincubated with 100 μM AG for 30 min and stimulated with LPS for the indicated

times. As shown in Figure 5A, phosphorylation of ERK and p38 was attenuated by AG, while that of JNK was unaffected. In addition, AG did not inhibit IκBα phosphorylation in LPS-stimulated RAW 264.7 cells (Fig. 5B). Consistent with these results, activation-related phosphorylation of Akt and p85, an important event for NF-κB activation and translocation, was not altered by AG (data not shown). To further confirm that the inhibitory effect of AG on LPS-induced iNOS and COX-2 expression was due to its influence on the activation of ERK and P38 MAPK pathways, specific inhibitors of ERK (PD98059) and p38 MAPK kinase (SB203580) were used. As shown in Figure 5C, treatment of cells with these inhibitors decreased iNOS and COX-2 expression in LPS-stimulated RAW264.7 cells. Taken together, these results support our hypothesis that inhibition of AP-1 activation by AG is due to inhibition of ERK and p38 phosphorylation, but not PI3K/Akt.

3.5. AG prevents LPS-induced septic shock in mice

Because AG attenuates LPS-induced proinflammatory cytokine levels in macrophages *in vitro*, it is important to confirm the physiological function of AG in an animal model. An established model to study the efficiency of anti-inflammatory agents is septic shock caused by LPS, which triggers severe injury and mortality in mice. As shown in Figure 6A, animal treatment with LPS resulted in 100% lethality at 36 h post-injection. However, pretreatment with varying concentrations of AG for 2 h before LPS challenge reduced this lethality. Proinflammatory cytokines have been shown to be key mediators of septic shock in several models of endotoxemia. LPS injection markedly increased the levels of TNF-α and IL-1β in serum, but pretreatment with AG significantly decreased the production of these two proinflammatory

cytokines (Fig. 6B and C). Using a mouse model, these results demonstrate that AG also has anti-inflammatory activity *in vivo*.

4. Conclusions

AG, a flavone glycoside isolated from fruit husks of *J. sigillata* for the first time, effectively reduced inflammatory responses via downregulation of inflammatory-related gene expression through the suppression of AP-1 and MAPK signaling pathways in LPS-stimulated RAW 264.7 cells. Using an *in vivo* model, AG also protected against lethality in mice that was triggered by endotoxin administration. The current work indicated that AG from fruit husks of *J. sigillata* may be applied as supplemental and/or functional foods having a beneficial effect against inflammation. And the investigation laid a foundation for comprehensive exploring the industrial forest and its products.

Competing interests

The authors declare that there are no conflicts of interest.

Acknowledgments

This study was supported financially by Natural Science Foundation of the Higher Education Institutions of Jiangsu Province (14KJB550002 and 15KJB550001), Natural Science Foundation of Jiangsu Province (BK20150414), and National Natural Science Foundation of China (31271857 and 31170541).

Notes and references

1 R. Medzhitov, Origin and physiological roles of inflammation, *Nature*, 2008, **454**, 428–435.

2 T. K. Hyun, Y. J. Ko, E. H. Kim, I. M. Chung and J. S. Kim, Anti-inflammatory activity and phenolic composition of *Dendropanax morbifera* leaf extracts, *Ind Crops Prod.*, 2015, **74**, 263–270.

3 M. H. Pan, C. S. Lai and C. T. Ho, Anti-inflammatory activity of natural dietary flavonoids, *Food Funct.*, 2010, **1**, 15–31.

4 C.L. Hsu, S.C. Fang and G.C. Yen, Anti-inflammatory effects of phenolic compounds isolated from the flowers of *Nymphaea mexicana* Zucc., *Food Funct.*, 2014, **4**, 1216–1222.

5 S. B. Abramson, M. Attur, A. R. Amin and R. Clancy, Nitric oxide and inflammatory mediators in the perpetuation of osteoarthritis, *Curr Rheumatol Rep*, 2001, **3**, 535–541.

6 Y. G. Lee, B. M. Chain and J. Y. Cho, Distinct role of spleen tyrosine kinase in the early phosphorylation of inhibitorof κBα via activation of the phosphoinositide-3-kinase and Akt pathways, *Int. J. Biochem. Cell Biol.*, 2009, **41**, 811–821.

7 M. E. Van Dort, S. Galbán, H. Wang, J. Sebolt-Leopold, C. Whitehead and H. Hong, Dual inhibition of allosteric mitogen-activated protein kinase (MEK) and phosphatidylinositol 3-kinase (PI3K) oncogenic targets with a bifunctional inhibitor, *Bioorg. Med. Chem.*, 2015, **23**, 1386–1394.

8 P. N. Moynagh, The roles of Pellino E3 ubiquitin ligases in immunity, *Nat. Rev. Immunol.*, 2014, **14**, 122–131.

9 S. Wu, X. He, S. Qin, J. He, S. Zhang and D. X. Hou, Inhibitory effects of blue honeysuckle (*Lonicera caerulea L*) on adjuvant-induced arthritis in rats: Crosstalk of anti-inflammatory

and antioxidant effects, *J Funct Foods*, 2015, **17**, 514–523.

10 W. F. Chiou, M. J. Don, J. F. Liao and B. L. Wei, Psoralidin inhibits LPS-induced iNOS expression via repressing Syk-mediated activation of PI3K-IKK-IκB signaling pathways, *Eur J Pharmacol.*, 2011, **650**, 102–109.

11 Y. C. Lin, D. Y. Huang, C. L. Chu and W. W. Lin, Anti-inflammatory actions of Syk inhibitors in macrophages involve non-specific inhibition of toll-like receptors-mediated JNK signaling pathway, *Mol Immunol.*, 2010, **47**, 1569–1578.

12 A. M. Urbanska, X. Y. Zhang and S. Prakash, Bioengineered colorectal cancer drugs: orally delivered anti-inflammatory agents, *Cell Biochem Biophys.*, 2015, **72**, 757–769.

13 Y. Zhou, D. M. Boudreau and A. N. Freedman, Trends in the use of aspirin and nonsteroidal anti-inflammatory drugs in the general U.S. population, *Pharmacoepidemiol Drug Saf.*, 2014, **23**, 43–50.

14 W. Ma, F. Liu, Y. Y. Ding, Y. Zhang and N. Li, Four new phenanthrenoid dimers from *Juncus effusus* L. with cytotoxicand anti-inflammatory activities, *Fitoterapia.*, 2015, **105**, 83–88.

15 W. X. Yan, J. H. Zhang, Y. Zhang, D. L. Meng and D. Yan, Anti-inflammatory activity studies on the stems and roots of *Jasminum lanceolarium* Roxb, *J Ethnopharmacol.*, 2015, **171**, 335–41.

16 L. G. Zhou, D. Li, J. G. Wang, Y. S. Liu and J. Y. Wu, Antibacterial phenolic compounds from the spines of *Gleditsia sinensis* Lam, *Nat Prod Res.*, 2007, **21**, 283–291.

17 C. L. Si, L. Wu, T. Shen, X. F. Huang, Z. G. Du and X. D. Ren, Recovery of low-molecular weight galloyltannins from agricultural residue of *Juglans sigillata* Dode seed husks and

their tyrosinase inhibitory effect, *Bioresources*, 2014, **9**, 2226–2236.

18 H. Ito, T. Okuda, T. Fukuda, T. Hatano and T. Yoshida, Two novel dicarboxylic acid derivatives and a new dimeric hydrolyzable tannin from walnuts, *J. Agric. Food Chem.*, 2007, **55**, 672–677.

19 Q. Liu, P. Zhao, X. C. Li, M. R. Jacob, C. R. Yang, and Y. J. Zhang, New α-tetralone galloylglucosides from the fresh pericarps of *Juglans sigillata*, *Helv. Chim. Acta*, 2010, **93**, 265–271.

20 H. M. Chiang, T. J. Lin, C. Y. Chiu, C. W. Chang, K. C. Hsu, P. C. Fan and K. C. Wen, *Coffea arabica* extract and its constituents prevent photoaging by suppressing MMPs expression and MAP kinase pathway. *Food Chem. Toxicol*., 2011, **49**, 309–318.

21 W. Hu, G. Wang, P. Li, Y. Wang, C. L. Si, J. He, W. Long, Y. Bai, Z. Feng and X. Wang, Neuroprotective effects of macranthoin G from *Eucommia ulmoides* against hydrogen peroxide-induced apoptosis in PC12 cells via inhibiting NF-κB activation. *Chem. Biol. Interact*., 2014, **224**, 108–116.

22 T. Shen, X. Li, W. Hu, L. Zhang, X. Xu, H. Wu and L. Ji, Hepatoprotective effect of phenylethanoid glycosides from *Incarvillea compacta* against CCl_4-induced cytotoxicity in HepG2 cells. *J Korean Soc Appl Biol Chem*., 2015, **58**, 617–625.

23 T. Hase, K. Ohtani, R. Kasai, K. Yamasaki and C. Picheansoonthon, Revised structure for hortensin, a flavonoid from *Millingtonia hortensis*, *Phytochemistry*, 1995, **40**, 287–290.

24 L. B. Roseiro, D. Viala, J. M. Besle, A. Carnat, D. Fraisse, J. M. Chezal and J. L. Lamaison, Preliminary observations of flavonoid glycosides from the vegetable coagulant *Cynara* L. in protected designation of origin cheeses, *Int Dairy J*, 2005, **15**, 579–584.

25 L. B. Rivera and G. Bergers, Intertwined regulation of angiogenesis and immunity by myeloid cells, *Trends Immunol.*, 2015, **36**, 240–249.

26 I. M. Sheldon, J. G. Cronin, G. D. Healey, C. Gabler, W. Heuwieser, and D. Streyl, Innate immunity and inflammation of the bovine female reproductive tract in health and disease, *Reproduction*, 2014, **148**, R41–R51.

27 R. Fuccelli, R. Fabiani, M. V. Sepporta, and P. Rosignoli, The hydroxytyrosol-dependent increase of TNF-α in LPS-activated human monocytes is mediated by PGE_2 and adenylate cyclase activation, *Toxicol In Vitro*, 2015, **29**, 933–937.

28 C. Bogdan, Nitric oxide synthase in innate and adaptive immunity: an update, *Trends Immunol.*, 2015, **36**, 161–178.

29 J. S. Shin, Y. M. Park, J. H. Choi, H. J. Park, M. C. Shin and Y. S. Lee, Sulfuretin isolated from heartwood of *Rhus verniciflua* inhibits LPS-induced induciblenitric oxide synthase, cyclooxygenase-2, and pro-inflammatory cytokines expression via the down-regulation of NF-κB in RAW 264.7 murine macrophage cells, *Int. Immunopharmacol.*, 2010, **10**, 943–950.

30 S. O. Abarikwu, Kolaviron, a natural flavonoid from the seeds of *Garcinia kola*, reduces LPS-induced inflammation in macrophages by combined inhibition of IL-6 secretion, and inflammatory transcription factors, ERK1/2, NF-κB, p38, Akt, p-c-JUN and JNK, *Biochim Biophys Acta.*, 2014, **1840**, 2373–2381.

31 J. Y. Kim, S. J. Park, K. J. Yun, Y. W. Cho, H. J. Park and K. T. Lee, Isoliquiritigenin isolated from the roots of *Glycyrrhiza uralensis* inhibits LPS-induced iNOS and COX-2 expression via the attenuation of NF-κB in RAW 264.7 macrophages, *Eur J Pharmacol.*,

2008, **584**, 175–184.

32 M. G. Djouossi, J. D. Tamokou, D. Ngnokam, J. R. Kuiate, L. A. Tapondjou and D. Harakat, Antimicrobial and antioxidant flavonoids from theleaves of *Oncoba spinosa* Forssk. (Salicaceae), *BMC Complement Altern Med.*, 2015, **15**, 134.

33 B. Y. Park, B. S. Min, S. R. Oh, J. H. Kim, K. H. Bae and H. K. Lee, Isolation of flavonoids, a biscoumarin and an amide from the flower buds of Daphne genkwa and the evaluation of their anti-complement activity, *Phytother Res.*, 2006, **20**, 610–613.

34 N. H. Yoo, D. S. Jang, J. L. Yoo, Y. M. Lee, Y. S. Kim and J. H. Cho, Erigeroflavanone, a flavanone derivative from the flowers of *Erigeron annuus* with protein glycation and aldose reductase inhibitory activity, *J Nat Prod.*, 2008, **71**, 713–715.

35 J. Wang, Y. T. Liu, L. Xiao, L. Zhu, Q. Wang and T. Yan, Anti-inflammatory effects of apigenin in lipopolysaccharide-Induced inflammatory in acute lung injury by suppressing COX-2 and NF-κB pathway. *Inflammation*., 2014, **37**, 2085–2090.

36 O. Farkas, O. Palócz, E. Pászti-Gere and P. Gálfi, Polymethoxyflavone apigenin-trimethylether suppresses LPS-induced inflammatory response in nontransformed porcine intestinal cell line IPEC-J2. *Oxid Med Cell Longev*., 2015, **2015**, Article ID 67384.

37 F. G. Miguel, A. H. Cavalheiro, N. F. Spinola, D. L. Ribeiro, G. R. M. Barcelos, L. M. G. Antunes, J. I. Hori, F. Marquele-Oliveira, B. A. Rocha and A. A. Berretta, Validation of a RP-HPLC-DAD method for chamomile (*Matricaria recutita*) preparations and assessment of the marker, apigenin-7-glucoside, safety and anti-inflammatory effect. *Evid Based Complement Alternat Med*., 2015, **2015**, Article ID 828437.

38 K. Newton and V. M. Dixit, Signaling in innate immunity and inflammation, *Cold Spring*

Harb Perspect Biol., 2012, **4**, 1–19.

39 S. M. Qi, Y. Q. Xin, Y. T. Guo, Y. Diao, X. J. Kou and L. Luo, Ampelopsin reduces endotoxic inflammation via repressing ROS-mediated activation of PI3K/Akt/NF-κB signaling pathways, *Int. Immunopharmacol.*, 2012, **12**, 278–287.

40 S. S. Boyanapalli, X. Paredes-Gonzalez, F. Fuentes, C. Zhang, Y. Guo and D. Pung, Nrf2 knockout attenuates the anti-inflammatory effects of phenethyl isothiocyanate and curcumin, *Chem Res Toxicol.*, 2014, **27**, 2036–2043.

41 W. J. Yoon, J. Y. Moon, G. Song, Y. K. Lee, M. S. Han, and J. S. Lee, *Artemisia fukudo* essential oil attenuates LPS-induced inflammation by suppressing NF-κB and MAPK activation in RAW 264.7 macrophages, *Food Chem Toxicol.*, 2010, **48**, 1222–1229.

42 Z. Y. Wun, C. F. Lin, W. C. Huang, Y. L. Huang, P. Y. Xu and W. T. Chang, Anti-inflammatory effect of sophoraflavanone G isolated from *Sophora flavescens* in lipopolysaccharide-stimulated mouse macrophages, *Food Chem Toxicol.*, 2013, **62**, 255–261.

43 W. J. Oh, U. Jung, H. S. Eom, H. J. Shin, and H. R. Park, Inhibition of lipopolysaccharide-induced proinflammatory responses by *Buddleja officinalis* extract in BV-2 microglial cells via negative regulation of NF-κB and ERK1/2 signaling, *Molecules*, 2013, **18**, 9195–9206.

44 S. H. Yang, A. D. Sharrocks and A. J. Whitmarsh, MAP kinase signalling cascades and transcriptional regulation. *Gene*., 2013, **513**, 1–13.

45 J. Y. Kwon, S. H. Hong, S. D. Park, S. G. Ahn, J. H. Yoon, B. M. Kwon and S. A. Kim, 2′-Benzoyloxycinnamaldehyde inhibits nitric oxide production in

lipopolysaccharide-stimulated RAW 264.7 cells via regulation of AP-1 pathway. *Eur. J. Pharmacol*., 2012, **696**, 179–186.

46 L. A. Ridnour, R. Y. Cheng, C. H. Switzer, J. L. Heinecke, S. Ambs and S. Glynn, Molecular pathways: Toll-like receptors in the tumor microenvironment—poor prognosis or new therapeutic opportunity, *Clin Cancer Res.*, 2013, **19**, 1340–1346.

47 Z. P. Tang, Q. Z. Cui, Q. Z. Dong, K. Xu and E. H. Wang, Ataxia–telangiectasia group D complementing gene (ATDC) upregulates matrix metalloproteinase 9 (MMP-9) to promote lung cancer cell invasion by activating ERK and JNK pathways, *Tumour Biol.*, 2013, **34**, 2835–2842.

48 P. D. Ray, B. W. Huang and Y. Tsuji, Reactive oxygen species (ROS) homeostasis and redox regulation in cellular signaling, *Cell Signal*, 2012, **24**, 981-990.

49 B. Hoesel and J. A. Schmid, The complexity of NF-κB signaling in inflammation and cancer, *Mol Cancer.*, 2013, **12**, 86.

50 J. Chun, R. J. Choi, S. Khan, D. S. Lee, Y. C. Kim and Y. J. Nam, Alantolactone suppresses inducible nitric oxide synthase and cyclooxygenase-2 expression by down-regulating NF-κB, MAPK and AP-1 via the MyD88 signaling pathway in LPS-activated RAW 264.7 cells, *Int. Immunopharmacol.*, 2012, **14**, 375–383.

51 M. Endale, S. C. Park, S. Kim, S. H. Kim, Y. Yang and J. Y. Cho, Quercetin disrupts tyrosine-phosphorylated phosphatidylinositol 3-kinase andmyeloid differentiation factor-88 association, and inhibits MAPK/AP-1 andIKK/NF-κB-induced inflammatory mediators production in RAW 264.7 cells, *Immunobiology*, 2013, **218**, 1452–1467.

52 H. J. Lee, H. J. Lim, da Y. Lee, H. Jung, M. R. Kim and D. C. Moon, Carabrol suppresses

LPS-induced nitric oxide synthase expression by inactivation of p38 and JNK via inhibition of I-κBα degradation in RAW 264.7 cells, *Biochem Biophys Res Commun.*, 2010, **391**, 1400-1404.

53 M. J. Sung, M. Davaatseren, W. Kim, S. K. Park, S. H. Kim, and H. J. Hur,. Vitisin A suppresses LPS-induced NO production by inhibiting ERK, p38, and NF-κB activation in RAW 264.7 cells, *Int. Immunopharmacol.*, 2009, **9**, 319–323.

54 D. J. Kwon, S. M. Ju, G. S. Youn, S. Y. Choi and J. Park, Suppression of iNOS and COX-2 expression by flavokawain A via blockade of NF-κB and AP-1 activation in RAW 264.7 macrophages, *Food Chem Toxicol.*, 2013, **58**, 479–486.

55 K. N. Kim, S. J. Heo, W. J. Yoon, S. M. Kang, G. Ahn, and T. H. Yi, Fucoxanthin inhibits the inflammatory response by suppressing the activation of NF-κB and MAPKs in lipopolysaccharide-induced RAW 264.7 macrophages, *Eur J Pharmacol.*, 2010, **649**, 369–375.

56 Y. M. Kim, H. J. Kim and K. C. Chang, Glycyrrhizin reduces HMGB1 secretion in lipopolysaccharide-activated RAW 264.7 cells and endotoxemic mice by p38/Nrf2-dependentinduction of HO-1, *Int. Immunopharmacol.*, 2015, 26, 112–118.

57 E. J. Park, S. W. Park, H. J. Kim, J. H. Kwak, D. U. Lee and K. C. Chang, Dehydrocostuslactone inhibits LPS-induced inflammation by p38MAPK-dependent induction of hemeoxygenase-1 *in vitro* and improves survival of mice in CLP-induced sepsis *in vivo*, *Int. Immunopharmacol.*, 2014, **22**, 332–340.

Figure legends:

Figure 1. Chemical structure of AG.

Figure 2. *In vitro* anti-inflammatory effect of AG in LPS-activated RAW 264.7 cells. (A) RAW 264.7 cells were plated in 96-well plate and then exposed to different concentrations of AG for 24 h and the cell viability was determined using an MTT assay. (B–D) The RAW 264.7 cells were cultured with different concentrations of AG in the presence or absence of LPS (1 μg ml^{-1}) for 24 h. The levels of NO, PGE_2, and TNF-α in the culture supernatants were determined by Griess assays and ELISAs as described in Materials and Methods. Each value is the mean ± standard deviation (n=3). Values with the same color bars with the same superscript letters are not significantly different from each other at $p < 0.05$.

Figure 3. The effect of AG on iNOS, COX-2, and TNF-α expression in LPS-activated RAW264.7 cells. RAW264.7 cells were incubated with AG in the presence or absence of LPS (1 μg ml^{-1}) for 6 h. Semi-quantitative PCR (A) and real time-PCR (B) were performed to determine the mRNA level of each gene with gene-specific primer. Within a column, values with the same superscript letters are not significantly different from each other at $p < 0.05$.

Figure 4. Effect of AG on translocation of transcription factors. (A) RAW264.7 cells (5×10^6 cells ml^{-1}) pre-treated with AG for 30 min were stimulated in the presence or absence of lipopolysaccharide (LPS) (1 μg ml^{-1}) for indicated time. After preparation of the nuclear fraction, protein levels of c-Jun, c-fos, p65, lamin A/C, and β-tublin were determined by immunoblotting

analysis. RAW 264.7 cells co-transfected with the plasmid constructs activating protein luciferase (NF-κB) (B) or AP-1-luc (C) and β-gal (as a transfection control) were treated with the AG in the presence or absence of LPS for 12 h. Luciferase activity was determined by luminometry. Values with the same superscript letters are not significantly different from each other at $p < 0.05$.

Figure 5. Effect of AG on the upstream signaling activation of AP-1. RAW264.7 cells (5×10^6 cells ml^{-1}) pre-treated with AG for 30 min were stimulated in the absence or presence of lipopolysaccharide (LPS) (1 μg ml^{-1}) for the indicated times. After immunoblotting, the levels of phospho- or total MAPKs (ERK, p38, and JNK) (A) or IκBα (B) were identified based on their antibodies. (C) Inhibitory effects of specific inhibitors of ERK (PD98059) and p38 MAPK kinase (SB203580) on LPS-induced iNOS and COX-2 expression in RAW 264.7 cells. Cells were pre-treated with PD98059 or SB203580 and real time-PCR were performed to determine the mRNA level of each gene with gene-specific primer. Within a column, values with the same superscript letters are not significantly different from each other at $p < 0.05$.

Figure 6. *In vivo* anti-inflammatory activity of AG. Ten mice per group were intraperitoneally administered with vehicle only or AG (5 or 10 mg kg^{-1}) 2 h before LPS challenge (20 mg/kg, i.p.). (A) Survival rates were observed over the next 84 h. Serum samples were obtained from each mouse 12 h after LPS injection. The levels of TNF-α (B) and IL-1β (C) were estimated using standard kits. Values with the same superscript letters are not significantly different from each other at $p < 0.05$.

Fig. 1.

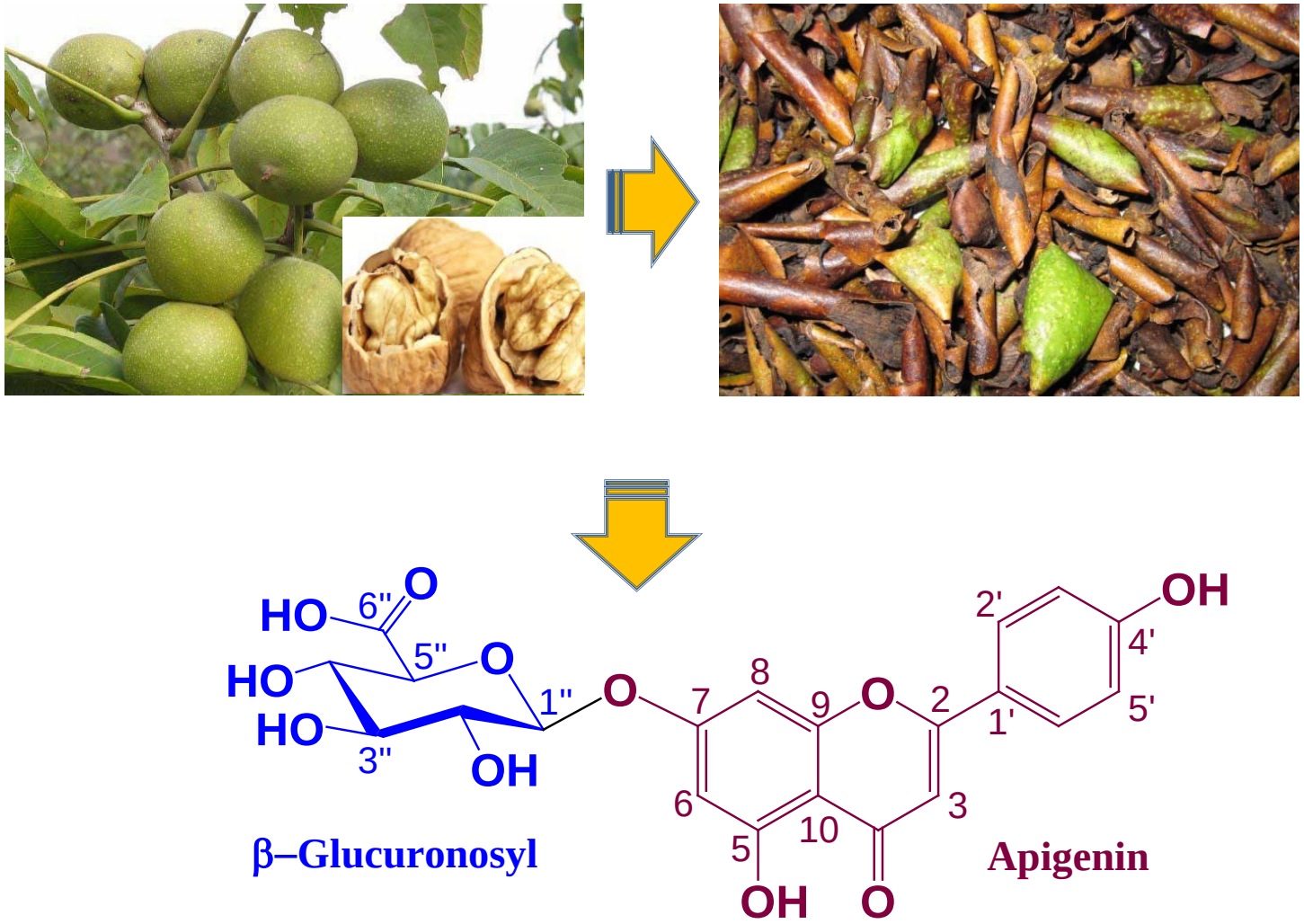

Apigenin-7-O-*β*-D-glucuronide (AG)

Fig. 2.

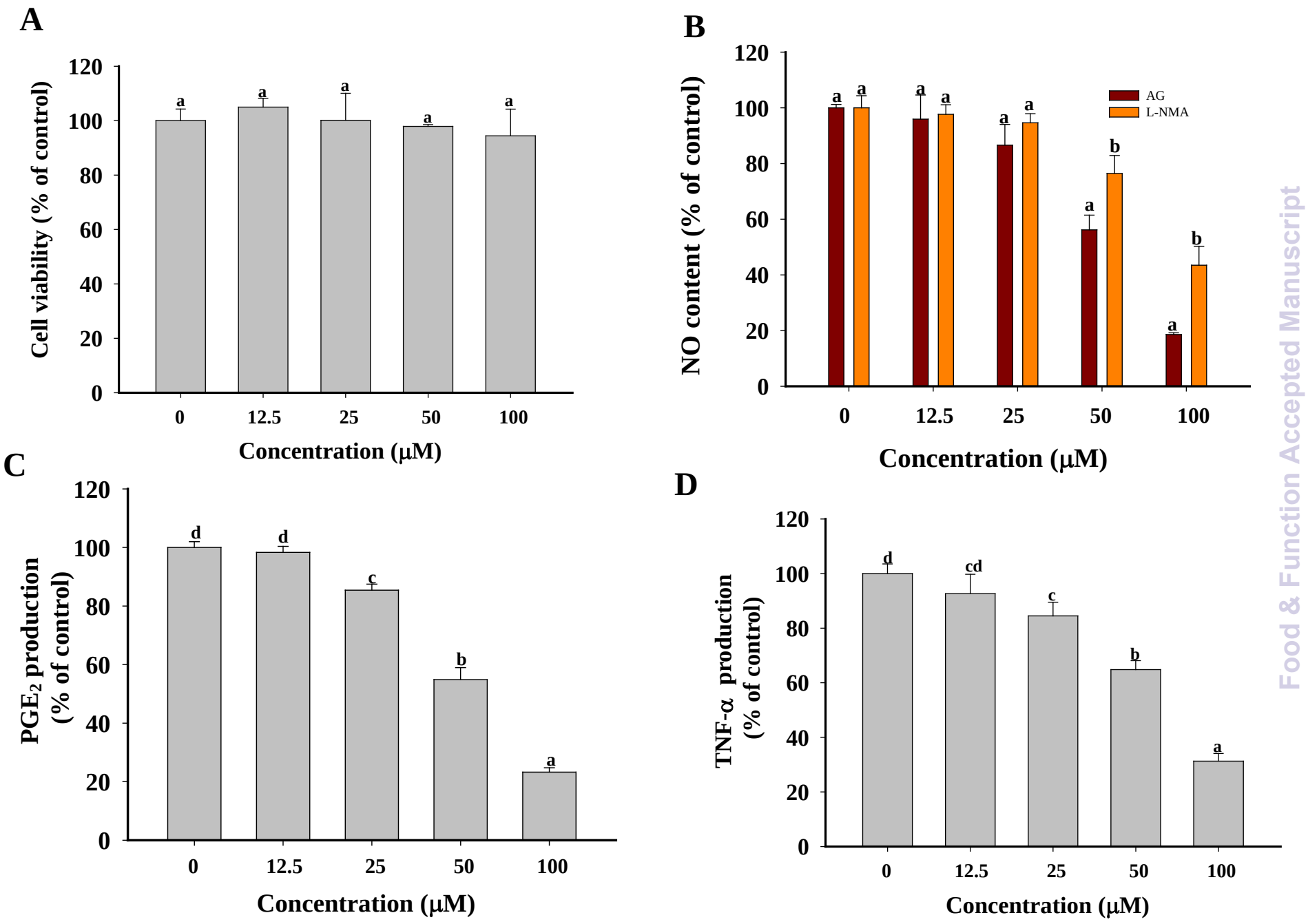

Fig. 3.

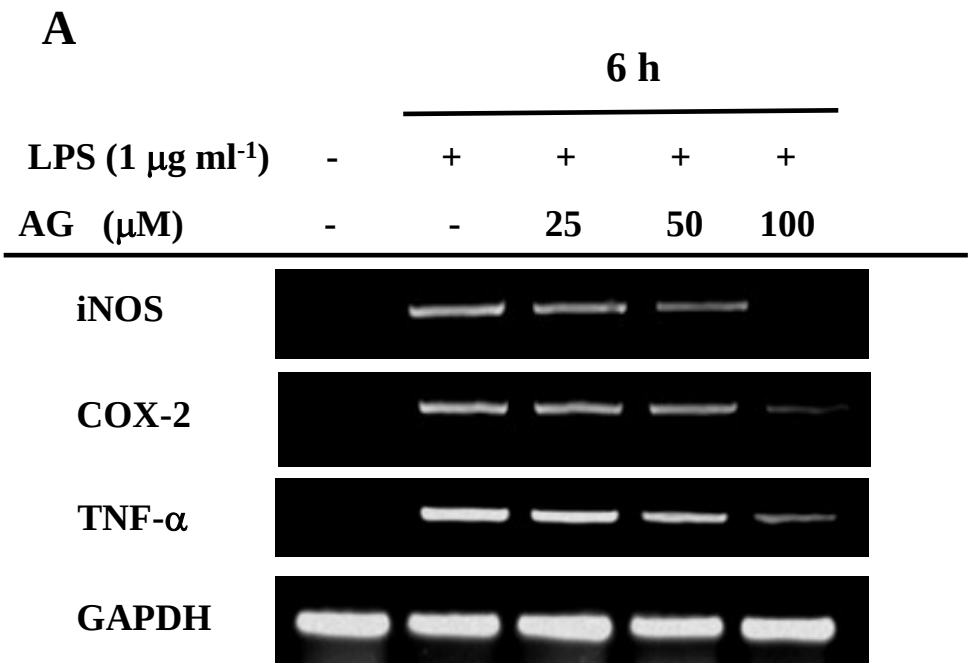

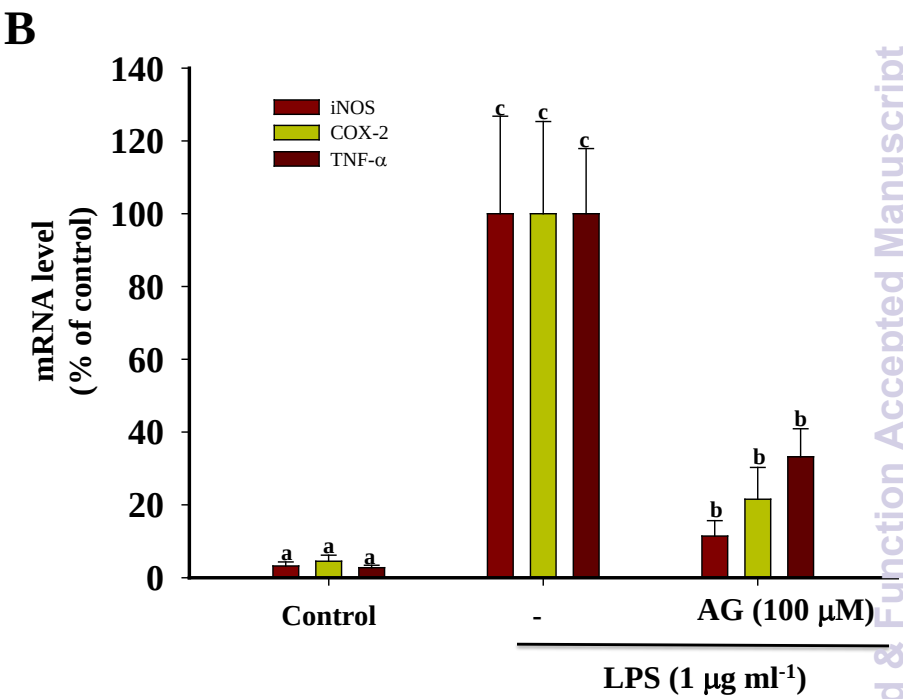

Fig. 4.

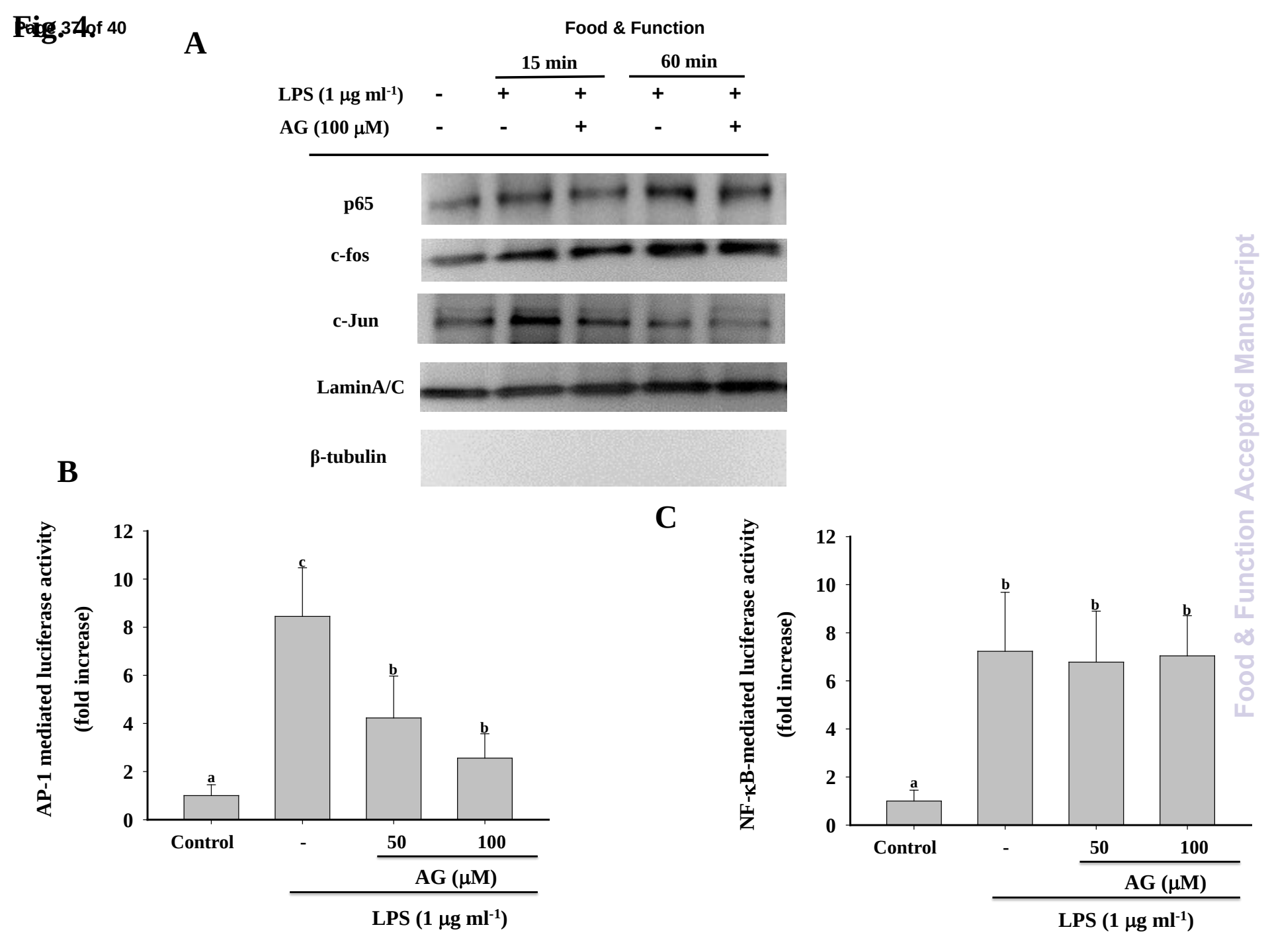

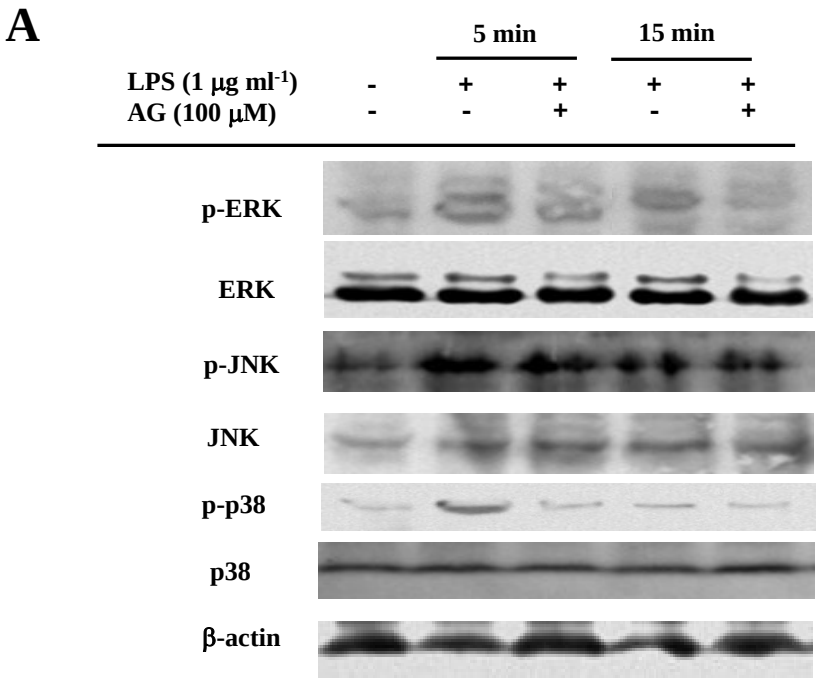

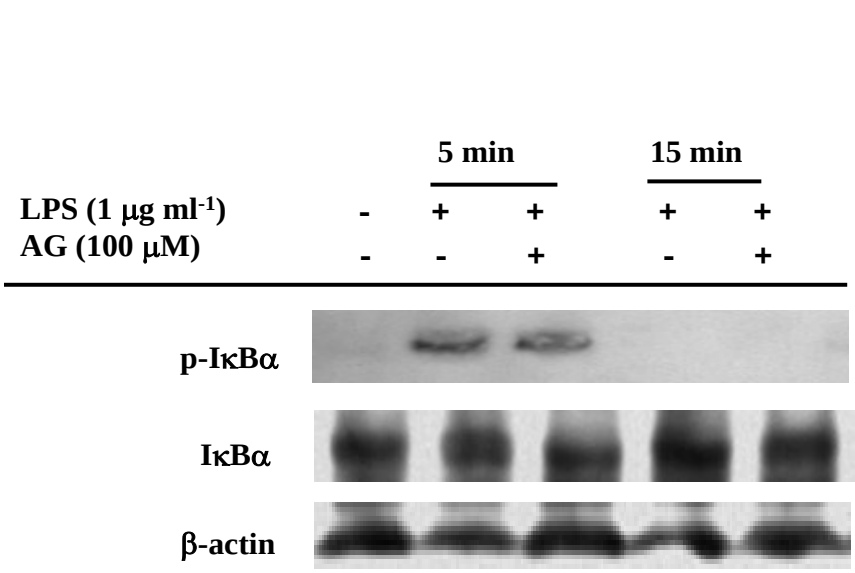

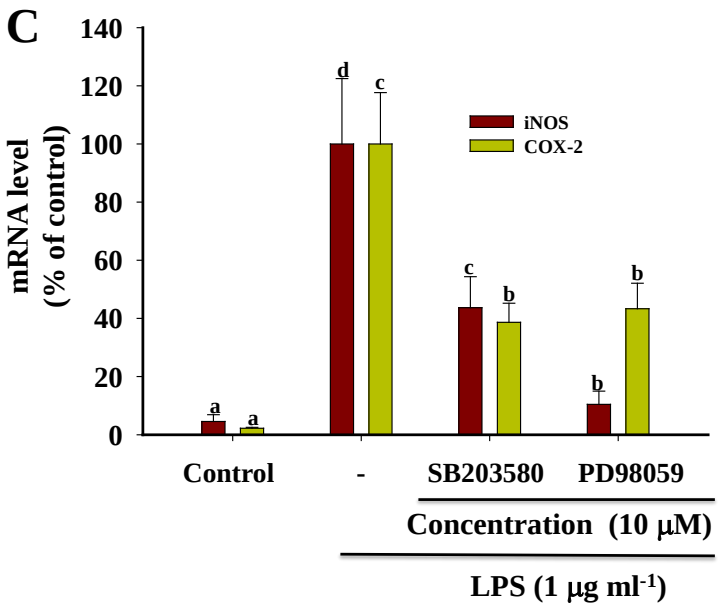

Fig. 6.

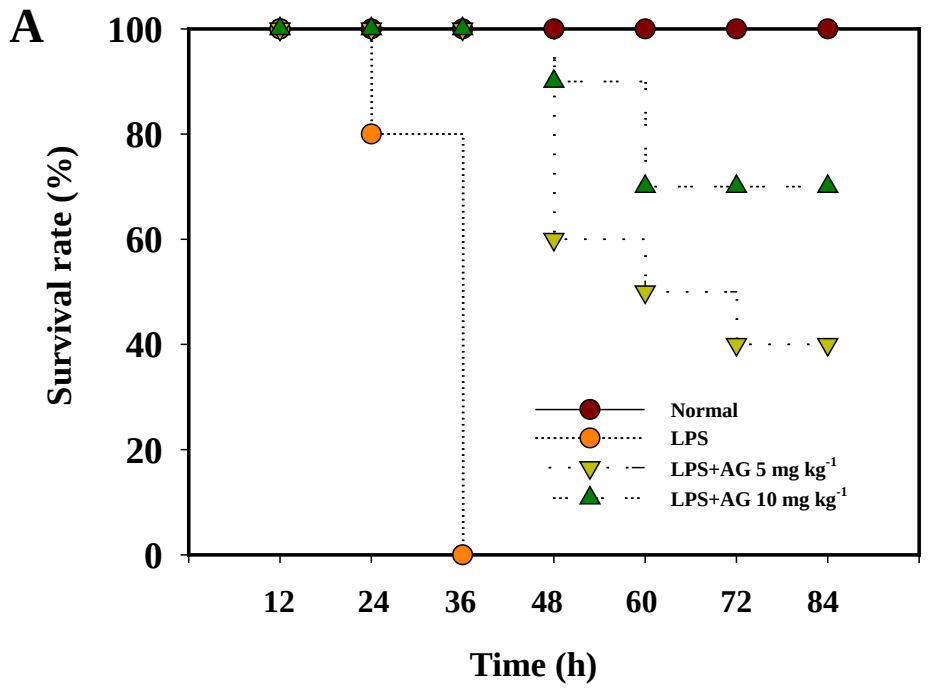

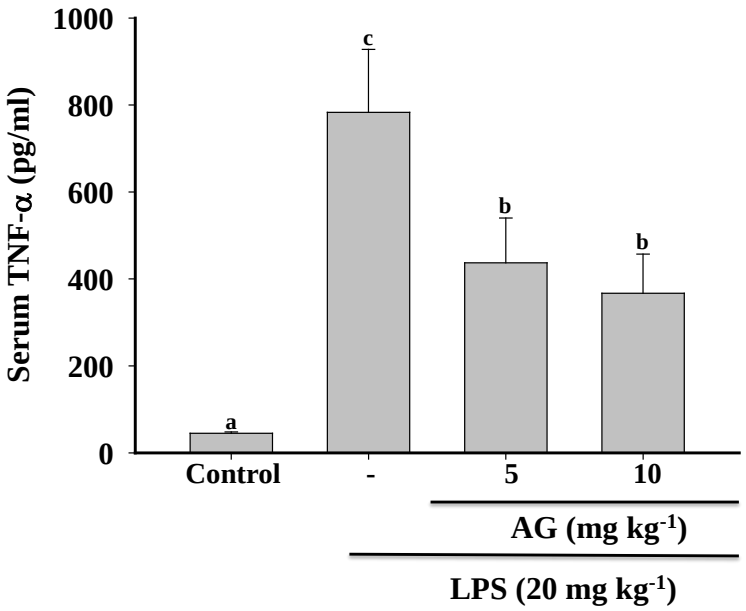

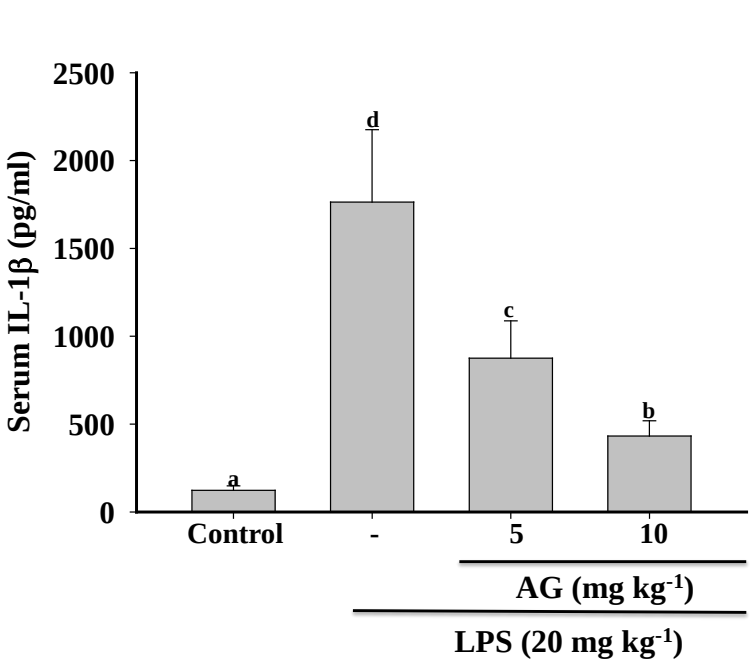

Graphic Abstract